

# Signal Transduction in Neuronal Migration: Roles of GTPase Activating Proteins and the Small GTPase Cdc42 in the Slit-Robo Pathway

Kit Wong,<sup>1,7</sup> Xiu-Rong Ren,<sup>3,7</sup> Yang-Zhong Huang,<sup>4</sup> Yi Xie,<sup>3</sup> Guofa Liu,<sup>1</sup> Harumi Saito,<sup>2</sup> Hao Tang,<sup>2</sup> Leng Wen,<sup>1</sup> Susann M. Brady-Kalnay,<sup>5</sup> Lin Mei,<sup>4</sup> Jane Y. Wu,<sup>2</sup> Wen-Cheng Xiong,<sup>3,6</sup> and Yi Rao<sup>1,6</sup>

<sup>1</sup>Department of Anatomy and Neurobiology

<sup>2</sup>Department of Pediatrics and Department of Molecular Biology and Pharmacology

Washington University School of Medicine  
660 South Euclid Avenue  
Saint Louis, Missouri 63110

<sup>3</sup>Department of Pathology

<sup>4</sup>Department of Neurobiology and Department of Pathology and Department of Physical Medicine and Rehabilitation

University of Alabama School of Medicine  
1530 3<sup>rd</sup> Avenue South  
Birmingham, Alabama 35294

<sup>5</sup>Department of Molecular Biology and Microbiology

Case Western Reserve University School of Medicine  
10900 Euclid Avenue  
Cleveland, Ohio 44106

## Summary

The Slit protein guides neuronal and leukocyte migration through the transmembrane receptor Roundabout (Robo). We report here that the intracellular domain of Robo interacts with a novel family of Rho GTPase activating proteins (GAPs). Two of the Slit-Robo GAPs (srGAPs) are expressed in regions responsive to Slit. Slit increased srGAP1-Robo1 interaction and inactivated Cdc42. A dominant negative srGAP1 blocked Slit inactivation of Cdc42 and Slit repulsion of migratory cells from the anterior subventricular zone (SVZa) of the forebrain. A constitutively active Cdc42 blocked the repulsive effect of Slit. These results have demonstrated important roles for GAPs and Cdc42 in neuronal migration. We propose a signal transduction pathway from the extracellular guidance cue to intracellular actin polymerization.

## Introduction

Extracellular cues guide the migratory direction of cells ranging from the bacteria to the social amoebae *Dictyostelium discoideum* to mammalian leukocytes (Devreotes and Zigmond, 1988). In the nervous system, although multiple families of guidance cues have been found in the last decade, our understanding of intracellular signal transduction mechanisms leading from the cell

membrane to the cytoskeleton remains limited (Mueller, 1999).

The Slit genes encode a family of secreted proteins that control the migration of neurons as well as leukocytes (Wu et al., 2001). First found in *Drosophila* (Nüsslein-Volhard et al., 1984; Rothberg et al., 1988), *slit* genes have also been identified in mammals, frogs, and chickens (Brose et al., 1999; Kidd et al., 1999; Li et al., 1999; Wang et al., 1999; Chen et al., 2001). Slit proteins can repel axons in *Drosophila* (Kidd et al., 1999; Batty et al., 1999) and in mammals (Brose et al., 1999; Li et al., 1999; Nguyen Ba-Charvet et al., 1999; Niclou et al., 2000; Erskine et al., 2000; Ringstedt et al., 2000). Slits can also promote axon branching (Wang et al., 1999) and repel migrating neurons (Wu et al., 1999; Zhu et al., 1999). Most recently, Slit has been found to inhibit leukocyte chemotaxis induced by chemotactic factors (Wu et al., 2001), suggesting a fundamental conservation of mechanisms guiding the migration of cells in diverse systems.

Genetic studies in *Drosophila* and biochemical studies in mammals have demonstrated that the Robos are receptors for the Slits (Brose et al., 1999; Kidd et al., 1999; Li et al., 1999). The extracellular part of each Robo contains five immunoglobulin (Ig) domains and three fibronectin type III (FNIII) repeats (Kidd et al., 1998; Zallen et al., 1998). The Ig domains in Robo are sufficient for mediating interaction with Slit (Chen et al., 2001; Nguyen Ba-Charvet et al., 2001). The intracellular part of Robo contains four identifiable motifs: CC0, CC1, CC2, and CC3 (Kidd et al., 1998; Zallen et al., 1998), and the functional significance of these motifs have been shown in *Drosophila* (Bashaw et al., 2000). The Abelson kinase (Abl) can phosphorylate a tyrosine residue in CC1 and downregulate Robo activity, whereas CC2 is a binding site for Enabled (Ena) (Bashaw et al., 2000). Our present studies of the CC3 motif have led to the finding of proteins regulating the Rho family of small guanosine triphosphatases (GTPases).

The Rho GTPases, particularly RhoA, Rac1, and Cdc42, play important roles in regulating the actin cytoskeleton (reviewed in Hall, 1998; Machesky and Insall, 1999). They have also been implicated in axon guidance and neurite outgrowth (reviewed in Luo, 2000). The GTP-bound forms of Rho GTPases are active, whereas the GDP-bound forms are inactive. The activities of Rho GTPases are regulated by GTPase activating proteins (GAPs) (reviewed in Lamarche and Hall, 1994), which increase the intrinsic GTPase activities, thus converting the GTP-bound forms to the GDP-bound forms. Rho GTPases are also regulated by guanine nucleotide exchange factors (GEFs), which exchange the GDP on an inactive GTPase for a GTP. In our efforts to study signal transduction mechanisms important for cell migration in the mammalian nervous system, we have discovered a family of GAPs that interact with the intracellular domain of Robo1. We present here biochemical and functional evidence for the involvement of GAPs and Cdc42 in mediating the repulsive response to Slit. We will discuss a pathway that leads from the extracellular interac-

<sup>6</sup>Correspondence: wxiong@path.uab.edu; raoyi@thalamus.wustl.edu

<sup>7</sup>These authors contributed equally to this work.

## A. Sequence of srGAP1 (KIAA1304)

```

MRVQLLQDLQDFFRKKAIEIETYSRNLEKLAERFMAKTRSTKDHQYKQDQNLSPVNCWYLLNQVRRESKDHTATLSDIYLNVMRFRMFIQSEDSTRMF 100
KKSKEIAFQHEHDLKMLNELYVMKTYHMYHAESISAESKLEAEKQEEKQIGRSGDPVPHIRLEERHQRRSSVKKIEKMKRQAKYSENKLSIKAR 200
NEVLLTLEATNASVFYIYHDSLDDCCDGLYHASLNALRRTYLSAEYNLETSRHEGLDIIENAVDNLEPRSDKQRFMEMYPAAFCCPPMKFFQSHMGD 300
EVCQVSAQQPVQAEMLMLRYQQLSRIATLKIENEVEVKKTTEATLQTIQDMVTIEDYDVSECFQHSRSTESVKSTVSETYLSKPSIAKRRANQQETEQFYF 400
MKLREYLEGNSLITKLQAKHDLQRTLGEGHRAEYMTTSRGRNRSHTRHQDSGQVIVPLIVESCIRFINLYGLQHQGIFRVSGSQVEVNDIKNSFERGENP 500
LADDQSNHDINSVAGVGLKLYFRLENLFPKERNFLDISCIRIDNLYERALHIRKLLTLPRSVLIVMRYLFAFLNHLSSQYSDENMMDPYNLAI CFGPTL 600
MPVPEIQDQVSCQAHVNEIKITIIHHETIFPDPAKELDGPVYKCMAGDDYCDSPYSEHGTLEEVDDQAGTEPHTSEDECEPIEAIKAFDYVGRSARELS 700
FKKGASLLYHRASEDWEGRHNGIDGLVPHQYIVVQDMDTDFDLSQKADSEASSGPVTEDKSSSKMNSPTDRHPDGYLARQRKRGEPPPVRPRGR 800
TSDGCHPLPHALSNSSVDLGSPLASHPRGLLQNRGNLNDSPERRRRRFGHGLTNI SRHDSLKIDSPPIRRSTSSGQYTFNDHKPLDPEITIAQDIE 900
ETMNTALNELRELERQSTAKHAPVVDLTLEQVKNSTPATSTESLPHHVALRSSEPIRRSTSSSDTMTSTFKPMVAPRMGVQLKPPALRPPKPAVLP 1000
TNPTIGPAPPQGGPTDKSCTM 1022
  
```

## B. FCH Domains

```

srGAP1  VQILLQDLQDFFRKKAIEIETYSRNLEKLAERFMAK---TRSTKDHQYKQDQNLSPVNCWYLLNQVRRESKDHTATLSDI
srGAP2  VQILLQDLQDFFRKKAIEIETYSRNLEKLAERFLAK---TRSTKD-QQFKKQDQNLSPVNCWYLLNQVRRESRDHTTILSDI
C1 rhoGAP  REILLQELAEFMRRAEVELEYSRGLKLAERFSSRGGRLGSSREHQSFRRKPESSLSPHLCWAVLLQHTRQQRSEAAISEV
CDC15   LSVLESIDPEYAKPASTERTYASKLDELAE-----SSADIPEVG-----SPLNNILSMRTETGSMKAHEEVSQQ
  
```

## C. RhoGAP Domains

```

srGAP1  VEVNDIKNSFERGENPLADDQSNHDINSVAGVGLKLYFRLENLFPKERNFLDISCIRIDNLYERALHIRKLLTLPRSVLIVMRYLFAFLNHLSSQ
srGAP2  VEVNDIKNAFERGEDPLAGDQNDHMDSTAGVGLKLYFRLENLFPKEDIFHDLACVITMDNLQERALHIRKVLVLPKTTLIIMRYLFAFLNHLSSQ
srGAP3  VEVNDIKNAFERGEDPLVDDQNERDINSVAGVGLKLYFRLENLFPKEREFDLSTIKLENPAERVHQIQQLVTLPRVIVVMRYLFAFLNHLSSQ
C1 rhoGAP  LRSFELRDAFERGEDPLVEGCTAHDLDSSVAGVGLKLYFRLENLFPPLFEPDLEBELLASSELEDTAERVEHVSRLVRLFAVVLVLYLFAFLNHLSSQ
  
```

```

srGAP1  YSDENMMDPYNLAI CFGPTLMPVPEIQDQVSCQAHVN
srGAP2  ESEENMMDPYNLAI CFGPSSMSVPEGHDDVBCDAHVN
srGAP3  ESEENMMDPYNLAI CFGPSSMHIIPDGDVBCDAHIN
C1 rhoGAP  YSDENMMDPYNLAI CFGPTLMPVPEIQDQVSCQAHVN
  
```

## D. SH3 Domains

```

srGAP1  684ATAKFDYVCRSARELDFKKGASLLYHRASEDWEGRHNGIDGLVPHQYIVV 735
srGAP2  757ATAKFDYVCRSARELDFKKGASLLYHRASEDWEGRHNGIDGLVPHQYIVV 808
srGAP3  300ATAKFDYVCRSARELDFKKGASLLYHRASEDWEGRHNGVDGLVPHQYIVV 351
C1 rhoGAP  751AVKCFAYTCRTAQELDFRRGDLVRLHERASSDWRGEHNGMRGLIPHYITL 802
CSK      14CTKYNFHTAEQDLDFCKGDLVLTIVAVTKDPNMYKAKKVKVGREGIIPANYV 65
  
```

## E.

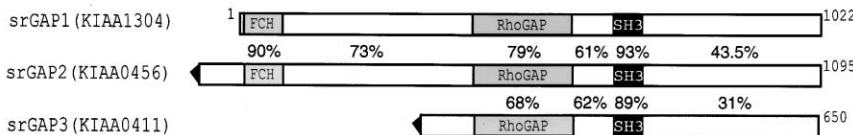


Figure 1. Sequences of srGAPs

(A) The primary sequence of the full-length srGAP1.

(B–D) Alignment of the FCH, SH3, and RhoGAP domains. Boxed are identical residues.

(E) A diagram of srGAPs 1, 2, and 3. The available sequences of srGAPs 2 and 3 are unlikely to be full-length because their 5' sequences do not have in-frame stop codons.

tion between Slit and Robo to the intracellular regulation of actin polymerization.

### Results

#### Identification of srGAPs as Robo Interacting Proteins

The yeast two-hybrid system was used to search for proteins interacting with the C-terminal region from amino acid residues (aa) 1455 to 1657 of rat Robo1. 20 positive clones were isolated from a mouse brain cDNA library, eight of which encoded a novel family of rhoGAP proteins named here as slit-robo (sr) GAPs 1, 2, and 3, corresponding to the human KIAA 1304, KIAA0456, and KIAA0411, respectively (Figure 1). The srGAPs contain an FCH domain, a rhoGAP domain, and an SH3 domain.

The FCH domain located from aa 11 to 110 in srGAP1 is similar to the FCH domains of srGAP2, srGAP3, C1 rhoGAP, cdc15, and Fer (Figure 1B). The centrally located rhoGAP domain (aa 483 to 657) in srGAP1 is highly similar to rhoGAP domains of srGAP2, srGAP3, and C1 rhoGAP (Figure 1C). The SH3 domain (aa 712 to 767) in srGAP1 is similar to those in srGAP2, srGAP3, C1 rhoGAP, and CSK (Figure 1D). The overall primary structures of the srGAP proteins are highly conserved (Figure 1E).

#### Expression Patterns of srGAPs and Interaction of Endogenous srGAP1 and Robo1

We first determined expression patterns of srGAP1 and srGAP2 mRNAs by Northern analysis. Three RNA transcripts of srGAP1 were detected at ~8.0, 5.5, and 3.8

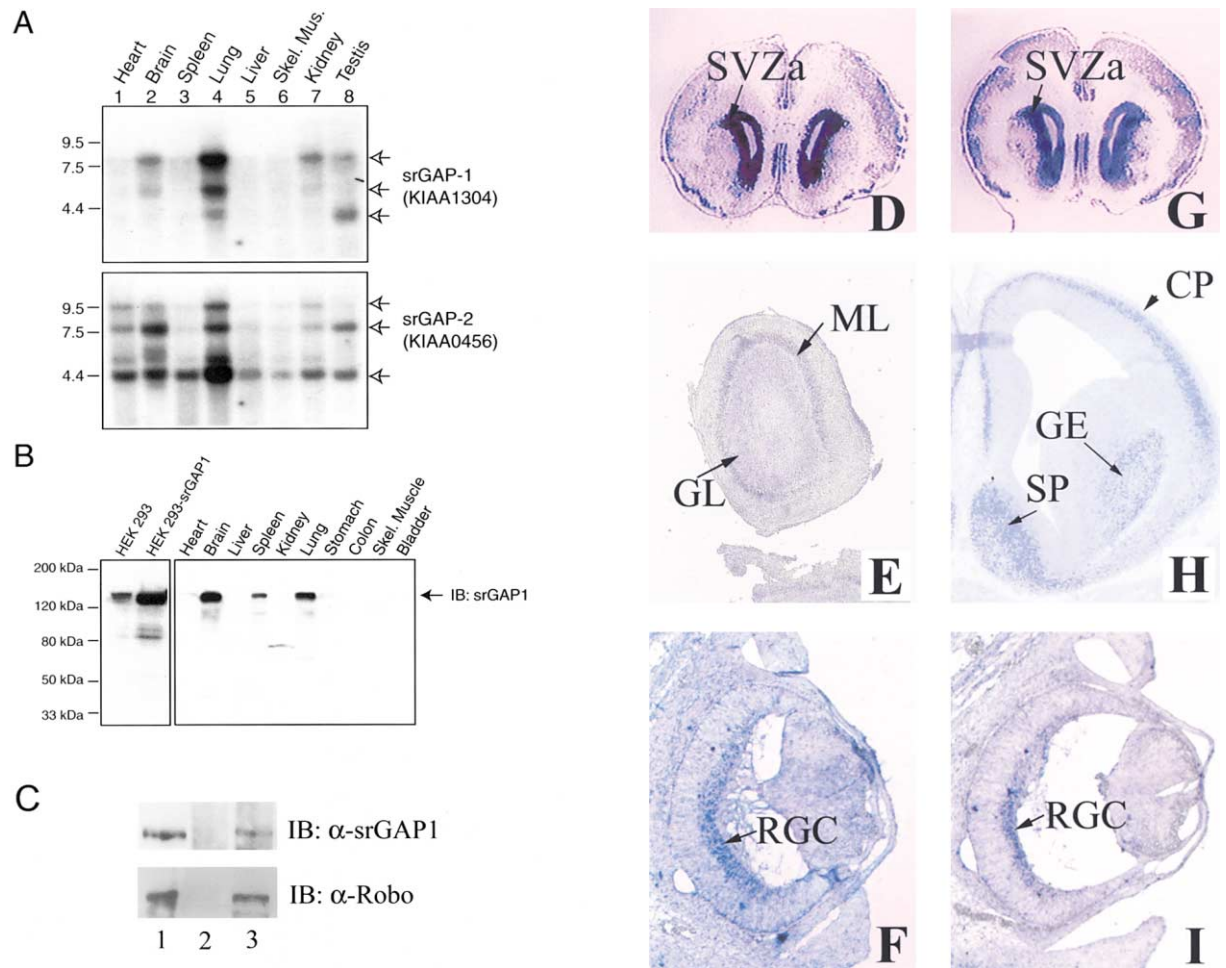


Figure 2. Expression of srGAPs and Interaction between Endogenous srGAP1 and Robo1

(A) Northern blot analyses. Molecular weight markers are indicated on the left in kb.

(B) Western blot analyses of srGAP1 were carried out using polyclonal anti-srGAP1 antiserum and lysates from HEK293 cells or lysates of various rat tissues.

(C) Coimmunoprecipitation of the endogenous srGAP1 and Robo1 proteins from primary neocortical cells of P1 rats. In the upper panel, lane 1: recognition of the endogenous srGAP1 by the anti-srGAP1 antibodies; lane 2: absence of srGAP1 in the immunoprecipitates pulled down by the preimmune serum; lane 3: presence of srGAP1 in the immunoprecipitates pulled down by the anti-Robo1 antibodies. In the lower panel, lane 1: recognition of endogenous Robo1 protein by the anti-Robo1 antibodies; lane 2: absence of Robo1 in the immunoprecipitates pulled down by the preimmune serum; lane 3: presence of Robo1 in the immunoprecipitates pulled down by the anti-Robo1 antibodies.

(D) srGAP1 expression in the SVZa shown in the coronal section of a postnatal day 3 (P3) rat brain.

(E) srGAP1 expression in the mitral cell layer (ML) and the granular cell layer (GL) of a P2 mouse olfactory bulb.

(F) srGAP1 expression in the RGC of an E15 mouse retina.

(G) Robo-1 expression in a section similar to that shown in (A) (P3 rat SVZa).

(H) srGAP2 expression in the coronal section of an E15 mouse telencephalon. Transcripts are detected in the differentiating field of the ganglion eminence (GE), in the septum (SP), and in the cortical plate (CP) of the neocortex.

(I) srGAP2 is also expressed in an E15 mouse retina.

kilobases (kb), with the 8.0 kb being the most abundant (Figure 2A). Three RNA transcripts of  $\sim$ 9.5, 8.0, and 4.4 kb were detected for srGAP2 with the 4.4 kb transcript as the most abundant (Figure 2A).

Western analysis with polyclonal antibodies against srGAP1 protein detected a band of approximately 130 kilodaltons (kDa) (Figure 2B). This band was recognized only by the srGAP1 antibodies, but not by the preimmune sera (data not shown). srGAP1 protein was expressed at high levels in the brain, the lung, and the spleen (Figure 2B). The relative expression levels of srGAP1 protein in different tissues were not identical to those of its mRNAs.

In situ hybridization on sections of rodent tissues was performed with digoxigenin-labeled probes to determine the distribution of srGAP mRNAs. srGAP3 was not detected in regions examined (data not shown), whereas srGAP1 and srGAP2 were found to be expressed in similar patterns; both were in regions responsive to Slit. In regions examined so far, the expression patterns of srGAP1 and 2 are very similar to that of Robo1 (Li et al., 1999; Yuan et al., 1999). Of particular interest to neuronal migration, precursor cells from the anterior subventricular zone (SVZa) of the neonatal forebrain are known to be repelled by Slit (Wu et al., 1999). Both srGAP1 and Robo1 were detected in the SVZa (Figures 2D and 2G).

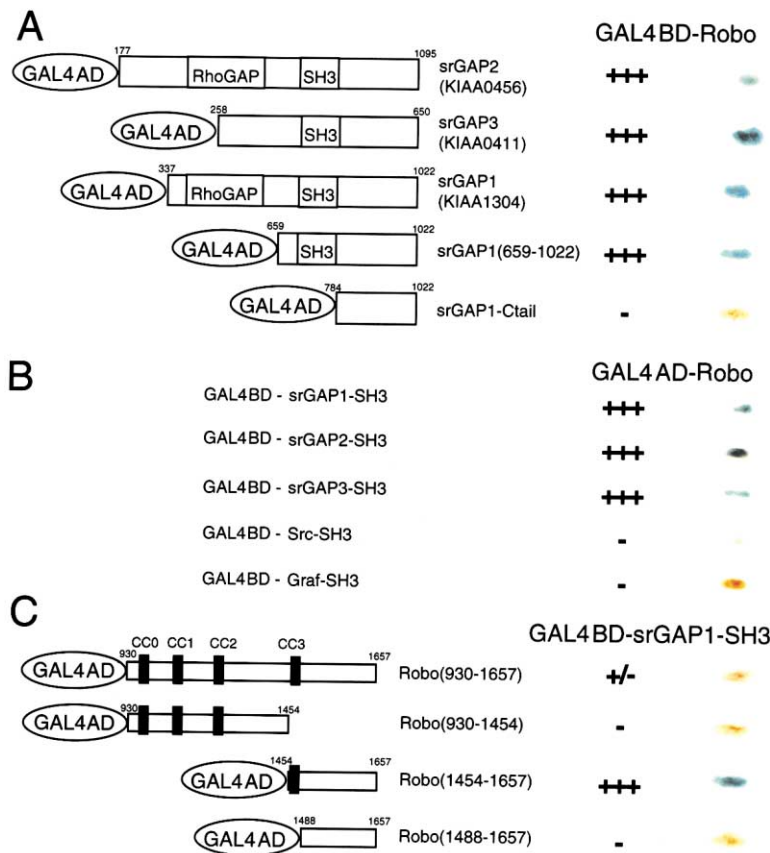


Figure 3. Interaction of Robo1 with srGAPs in the Yeast Two-Hybrid System

The scoring of  $\beta$ -Gal activity is as follows: (-): no blue color in the yeast after 24 hr in reaction; (+): yeast turning blue after 4 hr; (++) : appearance of blue color between 30 min to 4 hr and (+++) : yeast turning blue in approximately 30 min.

(A) Fragments in srGAPs were fused to the activation domain of Gal4 (GAL4AD), whereas the intracellular domain of Robo1 was fused to the DNA binding domain of Gal4 (GAL4BD). Deletion of the SH3 domain from srGAP1 eliminated its binding to Robo1.

(B) Robo1 specifically binds to SH3 domains in srGAPs but not to SH3 motif in Src or Graf. (C) The proline-rich motif in the CC3 region of Robo1 is necessary for its binding to the SH3 domain in srGAP1.

In regions relevant to axon guidance, srGAP1 and 2 were expressed in the olfactory bulb (Figure 2E) and in the retinal ganglion cells (RGCs) of E15 embryos (Figures 2F and 2I). srGAPs were expressed in the spinal cord and the dorsal root ganglia (DRG) (data not shown). They were also expressed in the cortical plate (CP) of the neocortex and in the mantle layer of the ganglionic eminence (GE, the striatal primordium) (Figure 2H). Neither Robo1 nor the srGAPs are in the subventricular zone of the GE to mediate the effect of Slit on cells migrating from the GE to the neocortex (Zhu et al., 1999). It remains to be determined whether other Robos and GAPs are expressed in the subventricular zone of the GE.

To examine potential interactions between the endogenous srGAP and Robo proteins, we prepared neocortical extracts from postnatal day 1 (P1) rats. Anti-Robo1 antibodies were used to precipitate proteins from primary cortical cells, and anti-srGAP1 antibodies were then used to detect srGAP1 in the immunoprecipitates. Results from coimmunoprecipitation experiments indicate that the endogenous srGAP1 and Robo1 proteins interacted with each other (Figure 2C). Taken together, these results have shown that srGAP1 and Robo1 are coexpressed in similar regions and that they interact in vivo.

#### Involvement of the SH3 Domain in srGAPs for Interaction with the CC3 Motif of Robo1

The domains responsible for srGAP1 interaction with the intracellular part of Robo1 were dissected with both yeast and mammalian systems. In the yeast (Figure 3A),

while proteins containing SH3 domains of srGAP1, 2, and 3 interacted with the intracellular region of Robo1, deletion of the SH3 domain (as in srGAP1-Ctail) eliminated the interaction of srGAP1 with Robo1. The SH3 domains in srGAPs were sufficient for binding to Robo (Figure 3B). Although it was reported previously that Robo1 could bind to the SH3 domain of Abl (Bashaw et al., 2000), Robo1 did not bind to the SH3 domains from Src or Graf, a rhoGAP domain containing protein interacting with the focal adhesion kinase (Hildebrand et al., 1996) (Figure 3B), indicating a preference of Robo1 for specific SH3 domains.

The dependence of the Robo1-srGAP1 interaction on the SH3 domain in srGAP1 suggests that the proline-rich sequences in Robo1 may be important. The intracellular part of Robo1 contains several proline-rich regions that are similar to the consensus SH3 binding site (Kidd et al., 1998; Zallen et al., 1998). While Robo1 protein containing the proline-rich CC3 motif (<sup>1481</sup>PPPPVPPP<sup>1488</sup>) [e.g., Robo (1454–1657)] interacted with the srGAP1 SH3 domain strongly, the deletion of the CC3 motif [in Robo (1488–1657) mutant] abolished the binding (Figure 3C). Results from the yeast two-hybrid system indicate that the SH3 domain in srGAPs and the proline-rich CC3 motif in the intracellular domain of Robo1 are essential for mediating their interaction.

To study the interaction between Robo1 and srGAP1 in mammalian cells, we made mutant forms of HA-tagged rat Robo1 (Figure 4A) and Flag-tagged srGAP1 (Figure 4B). They were transfected into human embryonic kidney (HEK) 293 cells, and protein-protein inter-

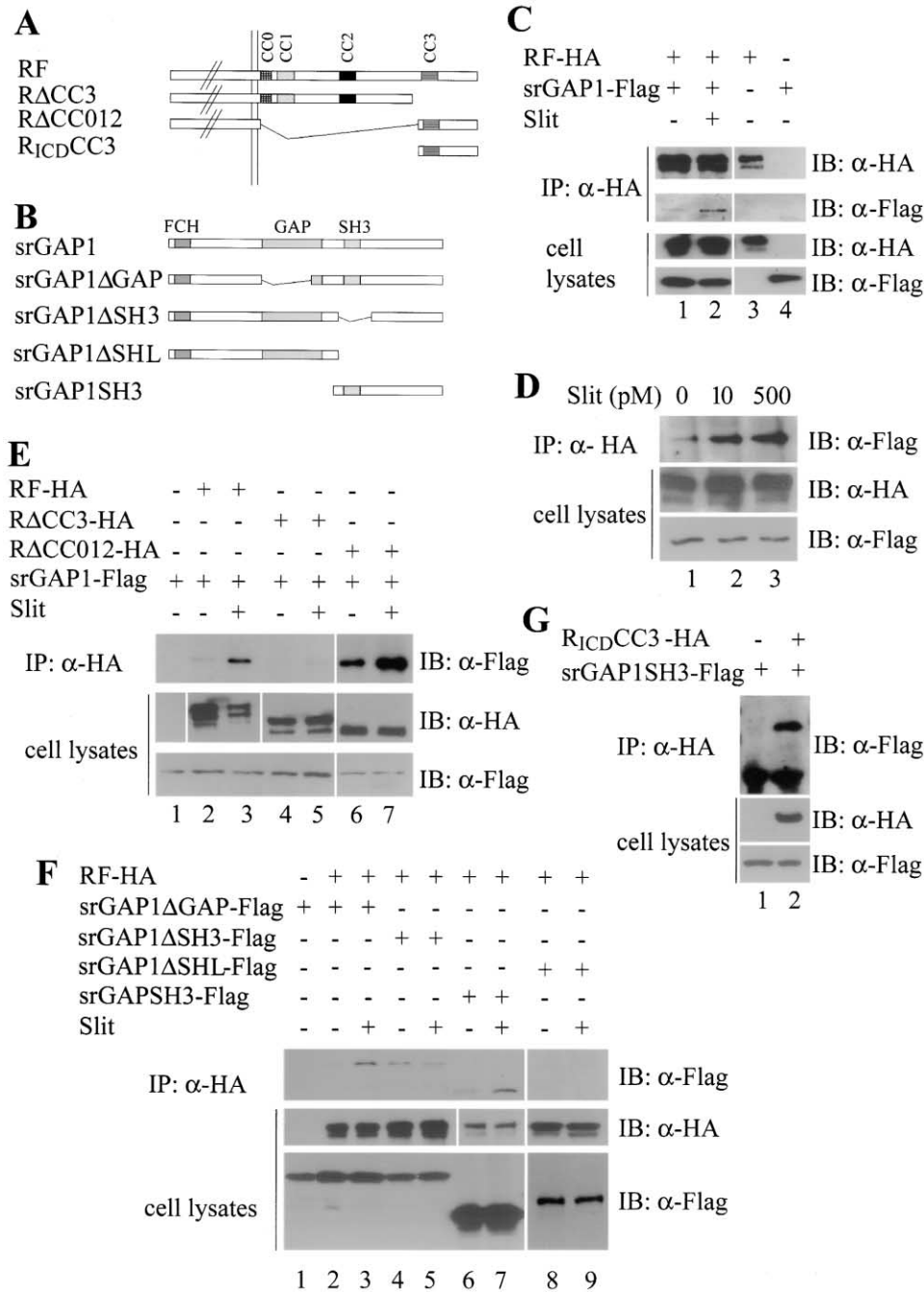


Figure 4. Interaction between srGAP1 and Robo1 in HEK Cells

Immunoprecipitation experiments were carried out to detect interactions of Flag-tagged srGAP1 mutants with HA-tagged Robo1 mutants. IP: antibodies used in immunoprecipitation; IB: antibodies used to analyze immunoblots.

(A) Diagrams of mutant forms of Robo1. RF: the full-length Robo. Residues 1455 to 1657 were deleted in R $\Delta$ CC3, and residues 930 to 1454 were deleted in R $\Delta$ CC012. R<sub>ICD</sub>CC3 contains residues 1455 to 1657.

(B) Diagrams of mutant forms of srGAP1. Residues 320 to 570 were deleted in  $\Delta$ GAP, residues 670 to 836 were deleted in  $\Delta$ SH3, and residues 674 to 1022 were deleted in  $\Delta$ SH3L. The srGAPSH3 fragment contains residues 624 to 1022 of srGAP1.

(C) Interaction between Robo1 and srGAP1. Immunoprecipitation was carried out with an anti-HA antibody. The first panel: Robo1 immunoprecipitated by anti-HA antibody was shown by the anti-HA antibody in the Western blot; the second panel: srGAP1 associated in the anti-HA Robo1 immunoprecipitate was detected by an anti-Flag antibody; the third and fourth panels show the specificities of the anti-HA and anti-Flag antibodies and the expression levels of Robo and srGAP1. In lane 2, HEK cells expressing Robo1 were treated with Slit for 5 min.

(D) Dosage-dependent regulation of srGAP1-Robo1 interaction by Slit.

(E) Interaction of full-length srGAP1 with various forms of Robo1. Deletion of CC3 dramatically reduced, but did not eliminate, Robo1 coimmunoprecipitation with srGAP1. Deletion of CC0, CC1, and CC2 led to increased interaction between Robo1 and srGAP1 (in R $\Delta$ CC012, lanes 6 and 7).

(F) Interaction of full-length Robo1 with mutant forms of srGAP1.

(G) The intracellular fragment of Robo1 containing the CC3 motif is sufficient for binding to the C-terminal region of srGAP1 containing its SH3 domain.

actions were studied by immunoprecipitation. The full-length srGAP1 was present in immunoprecipitates together with the full-length Robo1 (Figure 4C, lanes 1 and 2), whereas Flag-srGAP1 was not precipitated by the anti-HA antibody when Robo-HA was absent (Figure 4C, lanes 3 and 4).

When the SH3 domain in srGAP1 was deleted (as in srGAP1 $\Delta$ SH3), srGAP1 interaction with Robo1 was reduced, but not eliminated (Figure 4F, lane 4). When the sequence C-terminal to the SH3 domain was deleted together with the SH3 domain (as in srGAP1 $\Delta$ SH3L), interaction of srGAP1 with Robo1 was eliminated (Figure 4F, lane 8). The fragment containing the SH3 domain and its C-terminal sequence (in srGAP1SH3) was sufficient for interaction with Robo1 (Figure 4F, lane 6).

When the CC3 motif in Robo1 was deleted (as in R $\Delta$ CC3), Robo1 interaction with srGAP1 was significantly reduced, but not eliminated in HEK cells (Figure 4E, lane 4). The CC3 motif of Robo and its C-terminal sequence (as in R $\Delta$ CC012) were sufficient for interaction with the full-length srGAP1 (Figure 4E, lane 6). This interaction appeared to be stronger than that between the full-length Robo1 and the full-length srGAP1 (compare lane 6 to lane 2 in Figure 4E, with equivalent amounts of proteins used in coimmunoprecipitation). R<sub>co</sub>CC3, an intracellular fragment containing the CC3 motif of Robo1 and its C-terminal sequence, was sufficient for interaction with the fragment of srGAP1 containing the SH3 motif and its C-terminal sequence (as in srGAP1SH3) (Figure 4G).

There are apparent differences in the requirements of protein-protein interaction domains between those observed in the yeast two-hybrid system and those in the HEK cells. In the yeast, deletions of the Robo CC3 motif and the srGAP1 SH3 motif eliminated Robo1-srGAP1 interaction (Figures 3A and 3C). In HEK cells, deletion of both the SH3 domain and additional C-terminal sequence from srGAP1 is required to eliminate its interaction with Robo1 (Figure 4F, lane 6). Although the CC3 motif is sufficient for binding to srGAP1 in both the yeast and the HEK cells, deletion of CC3 did not eliminate Robo1-srGAP1 interaction in HEK cells (Figure 4E). One possibility is that more than one motif in Robo1 and srGAP1 is involved in their direct interaction in HEK cells, but not in the yeast nuclei. Another possibility is that regions in Robo1 and srGAP1 other than the CC3 and SH3 motifs can bring these proteins into complexes involving other proteins. In such a scenario, Robo1 and srGAP1 could be coimmunoprecipitated because they share common target proteins, which are present in mammalian cells, but absent from the yeast nuclei.

#### Slit Regulation of srGAP Interactions with Robo1 and Rho GTPases

To investigate whether the extracellular interaction between Slit and Robo can regulate the intracellular interaction between srGAP1 and Robo1, conditioned medium containing 200 pM of Slit2 protein was added to the medium culturing the Robo1-expressing HEK cells for 5 min before cell lysates were made. Slit significantly increased the binding of srGAP1 to Robo1 (Figure 4C, lane 2, compared to lane 1). This effect was dose-dependent in that increasing concentrations of Slit led to more

binding of srGAP1 with Robo1 (Figure 4D). These results indicate that extracellular Slit regulates the intracellular interaction between srGAP1 and Robo1.

When the SH3 domain in srGAP1 was deleted (as in srGAP1 $\Delta$ SH3), although srGAP1 could be immunoprecipitated with Robo1 (Figure 4F, lane 4), Slit could no longer upregulate the interaction of srGAP1 with Robo1 (Figure 4F, lane 5). When the SH3 domain and its C-terminal sequence were deleted (as in srGAP1 $\Delta$ SHL), no interaction between srGAP1 and Robo1 could be detected, regardless of the presence or absence of Slit (Figure 4F, lanes 8 and 9). Slit could upregulate the interaction between Robo1 and an srGAP1 fragment containing the SH3 domain and its C-terminal sequence (in srGAP1SH3) (Figure 4F, lanes 6 and 7). These results indicate that the SH3 domain in srGAP1 is necessary for Slit-regulated interaction between srGAP1 and Robo1.

When the CC3 motif was deleted from Robo1 (in R $\Delta$ CC3), Slit treatment did not increase the interaction between srGAP1 and Robo1 (Figure 4E, lanes 4 and 5). Slit could increase the interaction between srGAP1 and a Robo1 fragment containing CC3 and its C-terminal region but lacking CC0, CC1, and CC2 (in R $\Delta$ CC012) (Figure 4E, lanes 6 and 7). These results indicate that the CC3 motif in Robo1 is required for Slit-regulated srGAP1-Robo1 interaction.

To investigate whether srGAP1 could interact with the Rho GTPases, HEK cells stably expressing Robo1 were cotransfected with srGAP1 and constitutively active forms of myc-tagged RhoA, Rac1, and Cdc42. Immunoprecipitation with the anti-myc antibody followed by Western blotting with anti-Flag was used to detect interaction between srGAP1 and any one of the active forms of Rho GTPases (Figure 5A). Interaction of RhoA or Cdc42 with srGAP1 was detected using this assay (Figure 5A, lanes 5 and 9), but no interaction between Rac1 and srGAP1 was detected (Figure 5A, lanes 7–8). Slit was found to change the interaction between srGAP1 and Rho GTPases in an interesting manner: Slit increased srGAP1 interaction with Cdc42 (Figure 5A, lanes 9–10), but decreased srGAP1 interaction with RhoA (Figure 5A, lanes 5–6).

#### Regulation of Rho GTPase Activities by srGAPs and Slit

To assess the GTPase activating activity of srGAP1 in mammalian cells, we introduced srGAP1 into HEK cells together with the wild-type Rho GTPases. Glutathione-S-transferase (GST) fusion proteins were used in a GST pull-down assay to detect the levels of active GTPases. The GTP-bound active forms of Cdc42 and Rac1 were pulled down by a GST fusion protein of p21 binding domain of PAK1 (GST-PBD), whereas the GTP form of RhoA was pulled down by GST-Rhotekin (GST-RBD) (Sander et al., 1998; Ren et al., 1999). As shown in Figure 5B, coexpression of srGAP1 with the GTPases led to the reduction in the levels of active Cdc42 (lanes 4 and 5 in the top panel of Figure 5B) and RhoA (lanes 4 and 5 in the bottom panel of Figure 5B), but not Rac1 (lanes 4 and 5 in the middle panel of Figure 5B). These data demonstrated the specificity of srGAP1 in HEK cells: it inactivates only Cdc42 and RhoA, but not Rac1. When the rhoGAP domain was deleted from srGAP1 (in

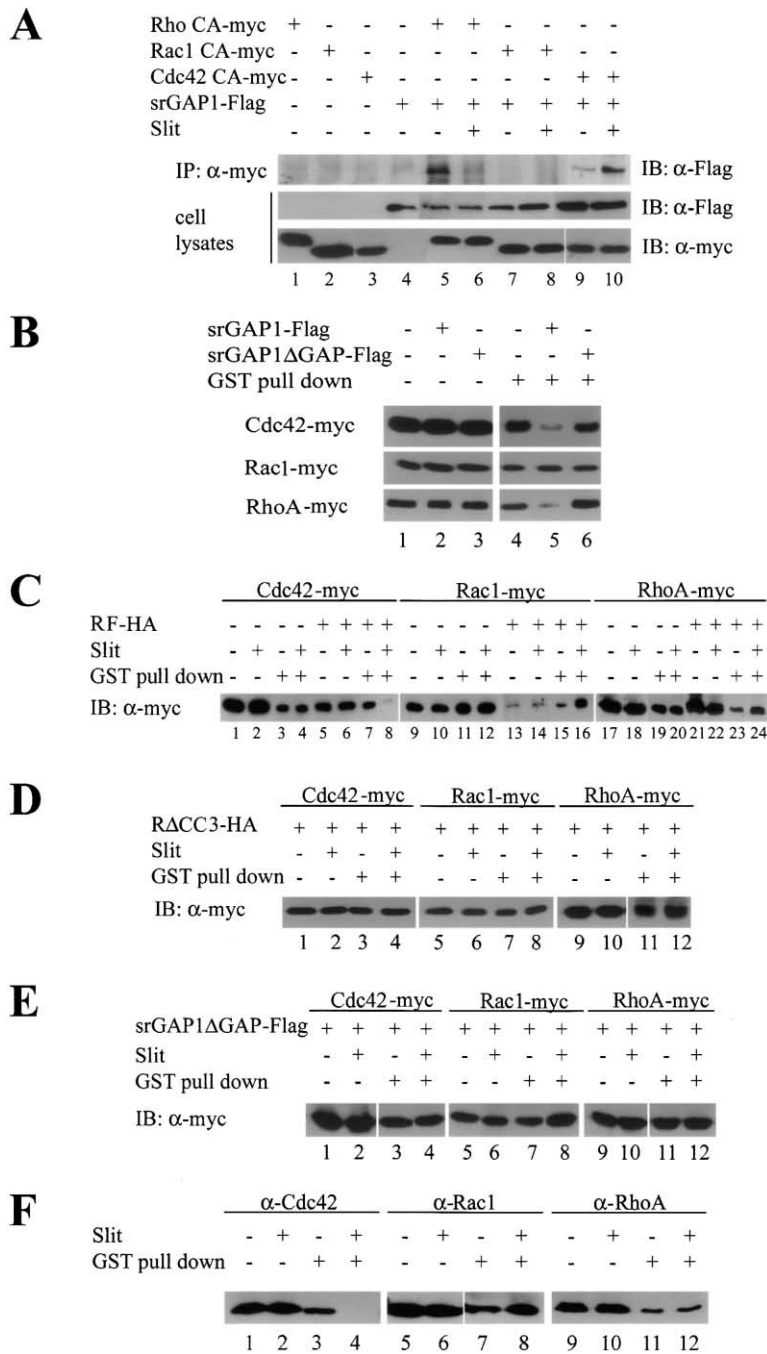


Figure 5. srGAP1 Interaction with and Regulation of Rho GTPases

(A) Biochemical interactions of srGAP1 with the constitutively active forms of the Rho GTPases were tested in Robo1-expressing HEK cells by coimmunoprecipitation. IP: antibodies used in immunoprecipitation; IB: antibodies used to analyze immunoblots.

(B) Regulation of RhoA, Rac1, and Cdc42 by srGAP1 and its mutant in HEK cells. GST fusion proteins of PBD- or RBD-conjugated beads were used to pull down GTP-bound forms of the Rho GTPases. Lanes 1, 2, and 3 are loading controls for the amount of myc-tagged GTPases in cell lysates before the pull-down experiments.

(C) Slit regulation of the Rho GTPases in control or Robo1-expressing HEK cells. In a Robo1-dependent manner, Slit decreased the level of active Cdc42, and increased the levels of active RhoA and Rac1.

(D) Inability of the Robo1 mutant lacking the CC3 motif (R $\Delta$ CC3) to mediate Slit regulation of Rho GTPases.

(E) The expression of the srGAP1 mutant lacking the GAP domain abolished Slit regulation of the activities of Cdc42 and RhoA, but not Rac1. Robo-1 expressing HEK cells were used in all lanes.

(F) Slit regulation of Rho GTPase activities in neonatal SVZa cells. The GST pull-down assay was carried out to measure the levels of GTP-bound forms of the endogenous Rho GTPases. After GST-pull down, the endogenous Rho GTPases were detected using corresponding specific antibodies. Lanes 1-2, 5-6, and 9-10 show loading of Cdc42, Rac1, and RhoA, respectively. Lanes 3, 4, 7, 8, 11, and 12 contain GST pull-down products.

srGAP1 $\Delta$ GAP), the mutant srGAP1 could no longer regulate the activities of Cdc42 or RhoA (lane 6 in all three panels of Figure 5B), indicating the requirement for the rhoGAP domain in the regulation of GTPase activities.

In HEK cells not expressing Robo1, Slit did not change the level of active Cdc42 (Figure 5C, lanes 1-4). However, in HEK cells expressing Robo1, Slit lowered the level of active Cdc42 (Figure 5C, lanes 5-8). These results indicate that the interaction between Slit and Robo1 leads to Cdc42 inactivation. The activities of both RhoA and Rac1 were increased by Slit stimulation of Robo1-expressing HEK cells (Figure 5C), although the increase in RhoA activity was modest. Because Slit acti-

vation of Rac1 is opposite to that expected of any direct effect of GAPs on Rho GTPases, and because direct binding was not detected between srGAP1 and Rac1 (Figure 5A), it is likely that the effect of Slit on Rac1 activity is not through srGAPs.

Data from HEK cells have demonstrated that CC3 and its C-terminal sequence in Robo1 are important for Slit regulation of Robo1 interaction with srGAP1 (Figure 4). We tested whether this region was essential for the Slit regulation of the Rho GTPases. R $\Delta$ CC3 was expressed in HEK cells and GST pull-down experiments were carried out after Slit treatment. The levels of active Cdc42, Rac1, and RhoA pulled down from cell lysates express-

ing this mutant Robo1 showed no difference with or without Slit (Figure 5D). These results indicate that the CC3 is necessary for the regulation of the Rho GTPases by Slit.

In the experiments described above (Figure 5C), Slit requires exogenously introduced Robo1 but not exogenous srGAP1 for its regulation of the Rho GTPases in HEK cells. This result is consistent with our finding of an endogenous srGAP1 in HEK cells (Figure 2B, lane 1). To determine whether the endogenous srGAP1 in HEK was involved in a step between Slit stimulation and GTPase regulation, we made use of the srGAP1 mutant without its rhoGAP domain (srGAP1 $\Delta$ GAP). This mutant was capable of binding to Robo1 in a Slit-regulated manner (Figure 4F, lanes 2 and 3), but lacked the ability to regulate the Rho GTPases (Figure 5B). It may therefore be a dominant negative form of the wild-type srGAP1. Introduction of srGAP1 $\Delta$ GAP into Robo1-expressing HEK cells blocked Slit regulation of the activities of Cdc42 and RhoA, but did not affect that of Rac1 (Figure 5E). These results are consistent with the earlier finding that srGAP1 did not regulate Rac1 (Figure 5B). Most importantly, together with the finding of srGAP1 expression in HEK cells, these results support the idea that srGAP1 is a critical link between Slit treatment and the regulation of Cdc42 and RhoA activities.

To investigate whether Slit regulates the activities of Rho GTPases in the nervous system, it was necessary to examine the activities of the endogenous Rho GTPases in regions responsive to Slit. Because the migration of neuronal precursor cells from the SVZa of the postnatal forebrain is guided by Slit (Wu et al., 1999; Hu, 1999), we tested whether Slit could change the levels of the GTP-bound forms of the endogenous Cdc42, Rac1, and RhoA in these cells (Figure 5F). SVZa cells were isolated and treated with Slit for 5 min before lysates were made for GST pull-down assays. Antibodies to Cdc42, RhoA, and Rac1 were used to detect the levels of the endogenous GTPases pulled down by the GST fusion proteins. Slit was found to decrease the level of the GTP-bound form of Cdc42 in SVZa cells (Figure 5F, lanes 3 and 4). These results indicate that Slit could regulate the activity of Cdc42 in primary cells in the nervous system, consistent with the results obtained from Robo1-expressing HEK cells.

In SVZa cells treated with Slit, a modest increase in the level of active Rac1 was detected (Figure 5F, lanes 7 and 8), whereas no significant change was observed in the level of active RhoA (Figure 5F, lanes 11 and 12). These results suggest that Robo1-expressing HEK and SVZa cells may share some common molecular components in mediating Slit-Robo signaling, at least in the regulation of Cdc42 and Rac1. In the case of RhoA, the difference between results from HEK and those from SVZa cells suggests that Slit regulation of RhoA activity is cell type-dependent.

#### **Involvement of Rho GTPases and srGAP1 in Mediating the Repulsive Response to Slit**

Because Slit regulates the activities of Rho GTPases, we investigated whether changes in the activities of the GTPases were functionally important for neuronal migration and for the repulsive response to Slit. We used dominant negative (DN) and constitutively active (CA)

forms of RhoA, Rac1, and Cdc42 to test for their involvement in guiding the migration of neuronal precursor cells from the SVZa. Taking advantage of the mitotic nature of the SVZa cells, we used retroviruses to introduce the mutant forms of the Rho GTPases.

Explants were isolated from neonatal rat SVZa and infected with a control retrovirus or retroviruses expressing mutant Rho GTPases. SVZa explants were then cocultured in the matrigel with aggregates of HEK cells secreting Slit (Wu et al., 1999). The effect of Slit was analyzed by observing the distribution of cells migrating from the SVZa explants and comparing the numbers of cells in the quadrant distal to the Slit aggregate with those in the proximal quadrant (Wu et al., 1999; Zhu et al., 1999).

SVZa cells infected with the control retrovirus were repelled by Slit, indicating that retroviral infection alone did not affect the Slit response (Figure 6A). Retroviruses expressing RhoA CA, Rac1 DN, or Cdc42 DN reduced the number of cells migrating from SVZa explants (Figures 6D, 6E, and 6G), indicating that SVZa cell migration was inhibited either by activation of RhoA or by inactivation of Rac1 or Cdc42. SVZa cells that did migrate in explants treated with these three mutants were still repelled by Slit. These results demonstrated that the activities of RhoA, Rac1, and Cdc42 could regulate neuronal motility. However, because cells that did migrate could be those with little or no expression of the mutant GTPases, these results could not conclusively answer the question of whether the Rho GTPases were involved in mediating the repulsive response to Slit.

The other three GTPase mutants (RhoA DN, Rac1 CA, and Cdc42 CA) did not inhibit neuronal migration (Figures 6C, 6F, and 6H). In fact, they all increased cell migration. In the cases of RhoA DN and Rac1 CA, migrating cells were still repelled by Slit. By contrast, cells from SVZa explants infected with Cdc42 CA migrated symmetrically around the circumferences of SVZa explants, indicating that Cdc42 CA specifically inhibited the repulsive effect of Slit (Figure 6H). Thus, reversal of the effect of Slit in reducing Cdc42 activity by Cdc42 CA blocked cellular responses to Slit. Taken together with our biochemical finding that Slit reduced Cdc42 activity, these results provide strong evidence supporting a role for Cdc42 in mediating the repulsive response of SVZa cells to Slit.

To test for a functional role of srGAP1 in SVZa cell migration, we used the srGAP1 mutant srGAP1 $\Delta$ GAP. This mutant was already shown to be defective in its GAP activity (Figure 5B) and could block the regulation of Cdc42 activity by Slit in HEK cells (Figure 5E). We made retroviral constructs expressing either srGAP1 $\Delta$ GAP or a control GFP protein. When the control vector was used to infect SVZa cells, SVZa cells were still repelled by Slit secreted from an aggregate of HEK cells (Figure 7A). After infection with the retrovirus expressing srGAP1 $\Delta$ GAP, SVZa cells were no longer repelled by Slit (Figures 7B and 7C). Taken together with the biochemical data, these results support the idea that srGAP1 functions in the Slit-Robo pathway.

#### **Discussion**

Our results indicate that srGAPs and Cdc42 are important components in the intracellular pathway mediating

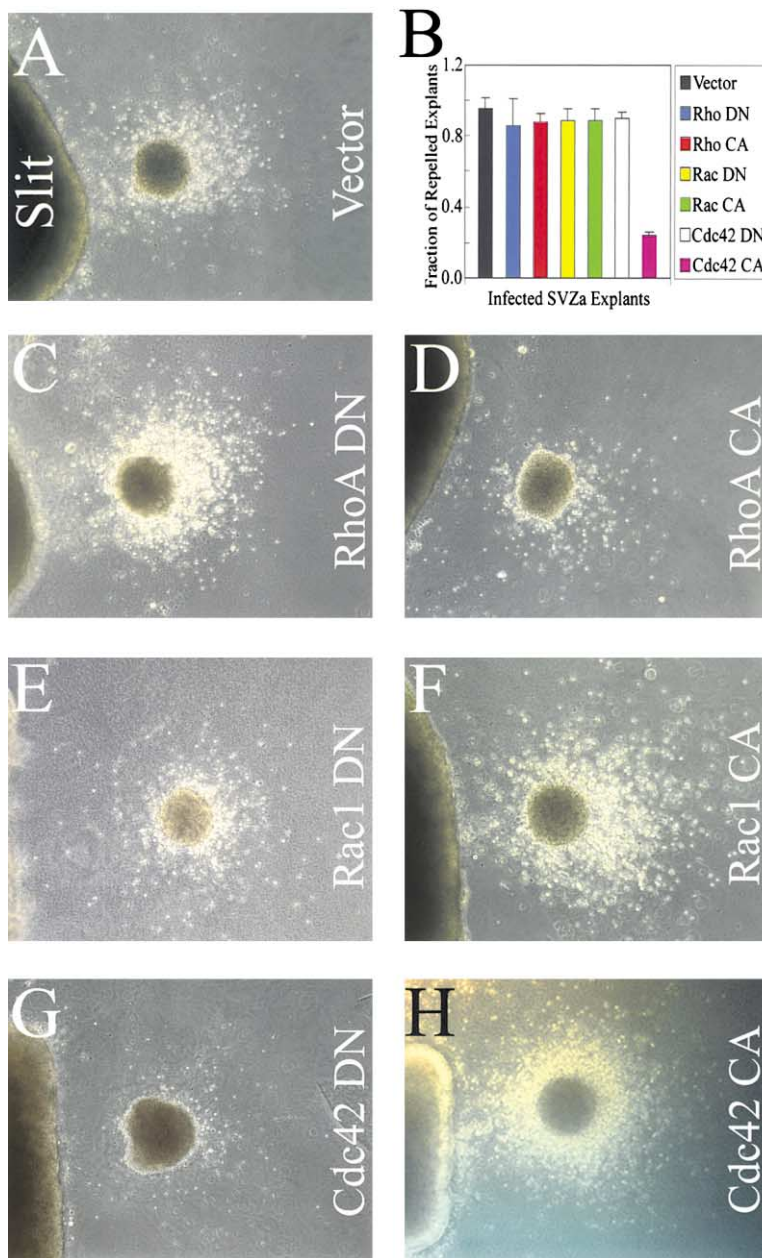


Figure 6. Functional Involvement of Rho GTPases in the Slit-Robo Pathway

An aggregate of HEK cells secreting Slit shown on the left part of each panel was cocultured with an SVZa explant. Dots surrounding each explant are migrating SVZa cells (Wu et al., 1999).

(A) Cells migrating out of the SVZa explants infected with a control retrovirus were repelled by Slit (60 out of 64 explants showing repulsion of SVZa cells).

(B) A diagram showing the statistical analysis of results from the coculture assays. The fractions of SVZa explants with cells repelled by Slit in each experiment were averaged and compared among the control ( $0.93 \pm 0.08$ ), RhoA DN ( $0.86 \pm 0.17$ ), RhoA CA ( $0.88 \pm 0.05$ ), Rac1 DN ( $0.88 \pm 0.08$ ), Rac1 CA ( $0.89 \pm 0.08$ ), Cdc42 DN ( $0.9 \pm 0.09$ ), and Cdc42 CA ( $0.24 \pm 0.04$ ).

(C) Results with SVZa explants infected with the retrovirus expressing a dominant negative RhoA. SVZa cells were repelled by Slit (with repulsion in 45 out of 53 explants).

(D) Results with SVZa explants infected with the constitutively active RhoA. Cell migration was reduced, but SVZa cells that did migrate were still repelled by Slit (repulsion in 45 out of 51 explants).

(E) Results with SVZa explants infected with the dominant negative Rac1. Cells that did migrate were still repelled by Slit (40 out of 46 repulsion).

(F) Results with SVZa explants infected with the constitutively active Rac1. SVZa cells were repelled by Slit (48 out of 54 repulsion).

(G) Results with SVZa explants infected with the dominant negative Cdc42. Migration of SVZa cells was reduced, but those cells that did migrate were still repelled by Slit (with repulsion seen in 63 out of 70 explants).

(H) Introduction of the constitutively active form of Cdc42 into SVZa explants inhibited the Slit-mediated repulsion of SVZa cells (19 out of 81 explants repelled).

the repulsive signaling of Slit and Robo. We propose here a pathway mediating Slit-Robo signaling (Figure 8). In this pathway, the leucine-rich regions of each Slit protein interact with the extracellular immunoglobulin domains of the Robo receptor (Chen et al., 2001; Nguyen Ba-Charvet et al., 2001). The extracellular interaction of Slit and Robo increases the interaction of the SH3 domain in an srGAP with the CC3 motif in Robo, resulting in localized activation of the srGAPs. srGAPs increase the intrinsic GTPase activity of Cdc42, which converts the GTP-bound form of Cdc42 into its GDP-bound form, therefore inactivating Cdc42. Inactivation of Cdc42 leads to a reduction in the activation of the Neuronal Wiskott-Aldrich Syndrome protein (N-WASP), thus decreasing the level of active Arp2/3 complex. Because active Arp2/3 promotes actin polymerization, the reduction of active Cdc42 eventually decreases actin polymer-

ization. The repulsive effect of Slit can therefore be explained by the relative amounts of actin polymerization on the sides of the cell proximal and distal to the Slit source, with the proximal side having relatively less actin polymerization than the distal side. Of course, this simple model needs to and can be adapted to the growth cones of projecting axons.

In this model, the part from the extracellular ligand to Cdc42 inactivation is supported by results presented in this paper. The part from Cdc42 to actin cytoskeleton is based on previous studies by others (Miki et al., 1996, 1998; Symons et al., 1996; Zigmund et al., 1997; Ma et al., 1998; Mullins and Pollard, 1999; Rohatgi et al., 1999, 2000; Higgs and Pollard, 2000; Prehoda et al., 2000). The last step of this pathway can be linked to the dendritic nucleation model of actin polymerization (Mullins et al., 1998; Blanchoin et al., 2000).

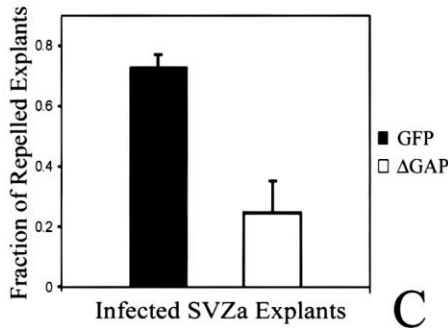
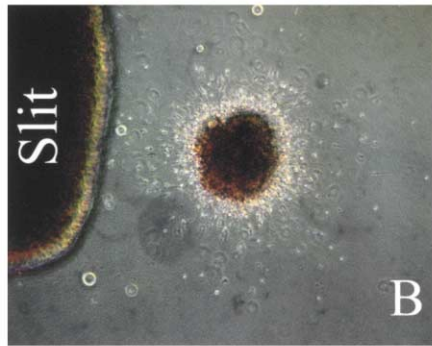


Figure 7. Inhibition of Slit Response by a Dominant Negative Mutant of srGAP1

(A) Repulsion of SVZa cells infected with control viruses (34 of 47 explants showing repulsion).  
 (B) Inhibition of a repulsive response in SVZa infected with srGAP1 mutant (with 27 of 108 explants showing repulsion).  
 (C) Quantitative analysis of coculture results. The fractions of SVZa explants with cells repelled by Slit were  $0.73 \pm 0.04$  for the GFP control and  $0.25 \pm 0.1$  for srGAP1 $\Delta$ GAP.

In addition to N-WASP, Slit regulation of Cdc42 may also inactivate Pak, a serine/threonine kinase that can be activated by Rac and Cdc42. Pak has been implicated in axon guidance in *Drosophila* (Hing et al., 1999). It is possible that there are multiple pathways used in temporally and spatially specific manners to guide neuronal migration. It is also possible that interaction of intracellular components determines the migratory behavior of axons and neurons. The pathway proposed here can serve as a working model for further experimental investigations.

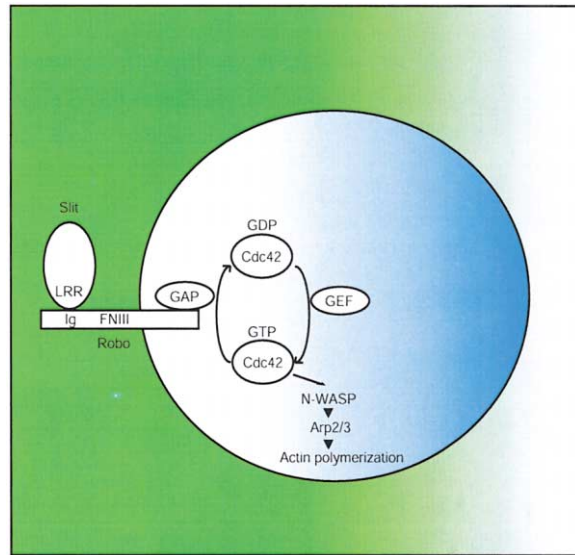


Figure 8. A Model for the Signal Transduction Pathway Mediating Slit Repulsion

A working hypothesis to explain how the extracellular Slit signal is transduced intracellularly, leading to the regulation of actin polymerization. The concentration of Slit on the left side of the cell is higher than that on the right side. Slit binding to Robo increases the GAP activity on the left side of the cell, hence more inactivation of Cdc42. Thus, on the left side of the cell, there will be less N-WASP activity, less Arp2/3 activity, and less actin polymerization. The asymmetry in actin polymerization on different sides of the cell causes it to move away from the source of Slit. The green gradation represents the extracellular gradient of Slit, whereas the blue gradation represents a hypothetical intracellular gradient of active Cdc42.

A large number of Rho GAPs have been identified. Our studies of srGAPs indicate that GAPs can regulate cell migration. The discovery of a variety of GAPs has led to the question why there are so many GAPs (Lamarque and Hall, 1994). The in situ hybridization results shown here suggest that some of the GAPs could be uniquely coupled to one or a few guidance receptors. Opposite to the GAPs, the GEFs activate GTPases. Recent studies in Eph signaling have revealed a role for a GEF in the EphrinA-EphA pathway (Shamah et al., 2001). EphrinA activates this GEF, which activates RhoA, leading to growth cone collapse. A role for GEFs in axon guidance is also known from studies of Trio, a GEF for Rac and Rho. *C. elegans* and *Drosophila* Trios play important roles in axon guidance and cell migration (reviewed in Lin and Greenberg, 2000). *Drosophila* Trio appears to act in the same pathway as Dreadlocks (Dock), an adaptor protein containing SH2 and SH3 domains (Garrity et al., 1996; Ruan et al., 2000), and Pak (Hing et al., 1999). Because the functionally important GEF domain of Trio activates only Rac, but not Cdc42 or Rho, it seems that Rac is the GTPase involved in this pathway. Vertebrate Trio has been found to be important in neural development (O'Brien et al., 2000), although it is not yet clear whether it is involved in axon guidance or neuronal migration.

Our results have demonstrated a role for Cdc42 in the migration of SVZa neurons, whereas the roles for RhoA and Rac1 are not yet clear. It remains possible that RhoA

and Rac1 can be involved in Slit-Robo pathway in a functionally important manner in certain cells. In HEK cells expressing Robo1, we have shown that srGAP1 can bind to the constitutively active forms of both RhoA and Cdc42, but not to Rac1. Interestingly, Slit treatment increases the interaction between srGAP1 and Cdc42, but decreases its interaction with RhoA. Furthermore, Slit inactivates Cdc42, but activates RhoA and Rac1. One explanation for Slit downregulation of Cdc42 is that Slit increases the binding of srGAP1 to Cdc42, which inactivates Cdc42. The simplest explanations for Slit regulation of RhoA in these HEK cells are that there is a high basal level of srGAP1 binding to and inactivating RhoA, and that Slit decreases the binding of srGAP1 to RhoA, which leads to a relative increase in RhoA activity.

In SVZa neurons, Slit also downregulates Cdc42 activity. Functionally, the dominant negative Cdc42 inhibits cell migration, whereas the constitutively active Cdc42 promotes cell migration and blocks the repulsive effect of Slit (Figure 6). The effect of the constitutively active Cdc42 is specific and not attributable to its promotion of cell migration or cell motility, because promotion of cell motility by dominant negative RhoA or constitutively active Rac1 could not block the repulsive activity of Slit on SVZa cells (Figure 6).

The functional role of RhoA in the Slit-Robo pathway is less clear in SVZa neurons. RhoA activity in SVZa neurons did not seem to be affected by Slit treatment. Although inhibition of neuronal migration by the constitutively active RhoA is consistent with a possible role for RhoA in Slit repulsion, a role for RhoA is not supported by the finding that dominant negative RhoA did not affect the repulsive effect by Slit. This is different from the involvement of RhoA in the ephrinA-EphA pathway (Wahl et al., 2000; Shamah et al., 2001).

So far there is no conclusive evidence to support a role for Rac1 in Slit signaling. Because srGAP1 does not bind to Rac1, Slit upregulation of Rac1 activity in HEK and SVZa cells is likely to be indirect. However, upregulation of Rac1 activity by the constitutively active Rac1 promoted the migration of SVZa neurons, making it unlikely that Rac1 is involved in the repulsive response to Slit, at least in SVZa neurons. Rac has been implicated downstream of plexins, the receptor for semas (Jin and Strittmatter, 1997; Kuhn et al., 1999; Vastrik et al., 1999; Vikis et al., 2000; Driessens et al., 2001).

Slit is also known to promote the branching of axons from the DRG (Wang et al., 1999) and growth cone collapse in RGC and olfactory bulb axons (Nguyen Ba-Charvet et al., 1999; Niclou et al., 2000). Because the actin cytoskeleton is likely to be involved in these processes, it is possible that Slit regulation of the Rho GTPases may underlie its activity in axon branching and growth cone collapse. The diversity of Slit effect observed in different tissues suggests that this ligand may have differential effects on the small GTPases in various cell types.

## Experimental Procedures

### Reagents

Rabbit antisera against srGAP1 were raised using a GST fusion protein containing residues 817 to 1022 of srGAP1. The anti-srGAP1 antibodies were purified by affinity column using srGAP1. Anti-

Robo1 antibodies were described previously (Wu et al., 2001). Monoclonal antibodies were purchased from Santa Cruz Biotechnology Inc. (anti-Myc; anti-RhoGTPases) and Sigma-Aldrich (anti-Flag).

### Yeast Two-Hybrid Screen and Assays

Several baits were designed to express different fragments of the intracellular domain of rRobo1 using pGBT9 vector (Clontech). The bait plasmid expressing residues 1455–1657 of robo1 was used as to screen a mouse brain cDNA library fused to the GAL4 transcriptional activation domain (kindly provided by Dr. Jeff Chamberlain) as described previously (Huang et al., 2000). The human KIAA0411, KIAA0456, and KIAA1304 clones were generously provided by Dr. Takahiro Nagase.

### Northern Analysis and In Situ Hybridization

To study mRNA distribution in different tissues, an RNA filter containing poly(A)<sup>+</sup> selected RNAs of multiple mouse tissues (Clontech) was hybridized with specific <sup>32</sup>P-labeled cDNAs. For in situ hybridization, mice and rats at embryonic day 15 and postnatal day 3 were used. Embryos and postnatal rodents were decapitated, and 8  $\mu$ m of serial sections were prepared and probed with digoxigenin (DIG) labeled probes.

### Constructs and Cell Lines

Full-length srGAP1 or srGAP2 were cloned into a mammalian expression vector under CMV promoter.

A plasmid expressing the full-length rat Robo1 protein in a HA-tagged form was constructed as described (Li et al., 1999). Deletion mutants of Robo1 were R $\Delta$ CC3 ( $\Delta$ 1455–1657) and R $\Delta$ CC012 ( $\Delta$ 930–1454), whereas R $\Delta$ CC3 contains residues 1455 to 1657. Deletion mutants of srGAP1 were srGAP1 $\Delta$ GAP ( $\Delta$ 320–570), srGAP $\Delta$ SH3 ( $\Delta$ 670–836), and srGAP $\Delta$ SH3L ( $\Delta$ 674–1022), whereas the SH3L fragment contains residues 624 to 1022 of srGAP1. Plasmids expressing wild-type, constitutively active (V12 Cdc42, V12 Rac1, and V14 RhoA) and dominant negative (N17 Cdc42, N17 Rac1, and N19 RhoA) Cdc42, Rac1, and RhoA as myc-tagged proteins were described previously (Ridley and Hall, 1992).

### RhoGAP Activity Assays

To test RhoGAP activity in vivo, GTP-loading of Cdc42, Rac1, or RhoA was determined by specific binding to the p21 binding domain of PAK1 (GST-PBD) or Rhotekin (GST-RBD) (Ren et al., 2001). Bound Cdc42, Rac1, or RhoA was analyzed by Western blotting using an anti-myc antibody (Babco).

To test for Slit regulation of Cdc42, Rac1, and RhoA activities, myc-tagged forms of wild-type Cdc42, Rac1, or RhoA were transfected alone or cotransfected with full length or mutant Robo-HA into HEK cells. 48 hr after transfection, cells were stimulated with conditioned medium of hSlit2-expressing HEK cells or 200 pM of purified hSlit2 in DMEM medium or medium alone at 37°C with 5% CO<sub>2</sub> for 5 min. Cell lysates were made and 9E10 anti-myc monoclonal antibody (Babco) was used in Western blot analysis to detect myc-tagged Cdc42, Rac1, or RhoA.

To detect Slit regulation of Cdc42, Rac1, and RhoA activities in primary neurons, explants of SVZa were dissected from P1–P5 rats, and were treated with conditioned media either from Slit-expressing HEK or from control HEK and lysed in RIPA buffer containing proteinase inhibitor. Antibodies to Cdc42, Rac1, and RhoA (Santa Cruz Biotechnology) were used to probe the blots with proteins pulled down by the GST fusion proteins.

### Retroviral Constructs and Neuronal Migration Assay

Construction and expression of the small G protein retroviruses was as follows. The retroviral system, generously provided by Steven Reeves (Harvard Medical School, Charleston, MA) is a tetracycline repressible promoter-based ("tet-off") system (Paulus et al., 1996). All of the necessary packaging genes and tetracycline regulatory proteins are found in the pBPSTR1 plasmid. The retroviruses used for our studies were made by transfecting the PA317 helper cell line with the corresponding plasmids to generate retroviruses that express various small G proteins. The following retroviral constructs were generated: dominant negative forms of the human isoforms

of the small G protein Cdc42 (T17N Cdc42), Rac1 (T17N Rac1), and RhoA (T19N RhoA), and the constitutively active forms of Cdc42 (Q61L Cdc42), Rac1 (Q61L Rac1), and RhoA (Q63L RhoA). We generated these constructs using DNA from plasmids generously provided by Lu-Hai Wang (Mount Sinai School of Medicine, NY) as templates for PCR, and added compatible flanking restriction sites in order to ligate the DNA into the pBPSTR1 vector.

Construction of retroviruses expressing srGAP1 was as follows. cDNA encoding srGAP1  $\Delta$ GAP was inserted between the BamHI and Sall sites of the pBMN-I-GFP vector. Retroviruses expressing GFP or srGAP1  $\Delta$ GAP fusion proteins were prepared by transfecting the corresponding retrovirus plasmids into amphotropic cells (Phoenix-Ampho) obtained from ATCC according to the instruction manual (Pear et al., 1997; Swift et al., 1999).

Retroviral infection into SVZa explants was performed essentially as described in Burden-Gulley and Brady-Kalnay (1999). SVZa explants were dissected from P1–P5 rats and were preincubated in retrovirus-containing F12 (10% FCS, 1% penicillin/Streptomycin, 5  $\mu$ g/ml polybrene) at 37°C with 5% CO<sub>2</sub>. After 18 hr of incubation, infected explants were cocultured with Slit aggregates in the matrix. Explants were photographed after 18–20 hr of culture using an Axioplan II microscope (Zeiss) equipped with a Spot video camera. The proportion of SVZa explants repelled was calculated from 9 independent experiments for vector control and Cdc42 CA and DN retroviruses. Statistical analyses of Rac1 and RhoA CA and DN samples were done on data from 5 independent experiments. Data on srGAP1 $\Delta$ GAP were collected from 4 independent experiments.

#### Acknowledgments

We are grateful to Elizabeth J. Rao for assistance; to Dr. J. Bamberg for adenoviral constructs; to Drs. Bernhard Mueller and John Collard for GST fusion proteins; Dr. Takahiro Nagase for KIAA plasmids; to Dr. Jeff Chamberlain for cDNA libraries; to Dr. Gary Nolan for providing the retrovirus system; to Adam Grasso and Jullia Rosdahl for assistance with the retroviruses; to the NIH (to Y.R., S.B.K., J.Y.W., and L.M.), the American Heart Association (Southeastern Division) (to W-C.X.), the Muscular Dystrophy Association and HHMI/UAB Faculty Development Award (to L.M.) for support; to the John Merck Fund, the Klingenstein Foundation, and the Leukemia Society of America for scholar awards (to Y.R. and J.Y.W.). We apologize for citation of reviews instead of original papers due to space constraints.

Received February 7, 2001; revised September 13, 2001.

#### References

Bashaw, G.J., Kidd, T., Murray, D., Pawson, T., and Goodman, C.S. (2000). Repulsive axon guidance: Abelson and Enabled play opposing roles downstream of the Roundabout receptor. *Cell* 101, 703–715.

Battye, R., Stevens, A., and Jacobs, J.R. (1999). Axon repulsion from the midline of the *Drosophila* CNS requires *slit* function. *Development* 126, 2475–2481.

Blanchoin, L., Amann, K.J., Higgs, H.N., Marchand, J.-B., Kaiser, D.A., and Pollard, T.D. (2000). Direct observation of dendritic actin filament networks nucleated by Arp2/3 complex and WASP/Scar proteins. *Nature* 404, 1007–1011.

Brose, K., Bland, K.S., Wang, K.H., Arnott, D., Henzel, W., Goodman, C.S., Tessier-Lavigne, M., and Kidd, T. (1999). Evolutionary conservation of the repulsive axon guidance function of Slit proteins and of their interactions with Robo receptors. *Cell* 96, 795–806.

Burden-Gulley, S.M., and Brady-Kalnay, S.M. (1999). PTP regulates N-Cadherin-dependent neurite outgrowth. *J. Cell Biol.* 144, 1323–1336.

Chen, J., Wen, L., Dupuis, S., Wu, J.Y., and Rao, Y. (2001). The N terminal leucine rich regions in Slit are sufficient to repel olfactory bulb axons and subventricular zone neurons. *J. Neurosci.* 21, 1548–1556.

Devreotes, P.N., and Zigmond, S.H. (1988). Chemotaxis in eukaryotic

cells: a focus on leukocytes and *Dictyostelium*. *Annu. Rev. Cell Biol.* 4, 649–686.

Driessens, M.H., Hu, H., Nobes, C.D., Self, A., Jordens, I., Goodman, C.S., and Hall, A. (2001). Plexin-B semaphorin receptors interact directly with active Rac and regulate the actin cytoskeleton by activating Rho. *Curr. Biol.* 11, 339–344.

Erskine, L., Williams, S.E., Brose, K., Kidd, T., Rachel, R.A., Goodman, C.S., Tessier-Lavigne, M., and Mason, C.A. (2000). Retinal ganglion cell axon guidance in the mouse optic chiasm: expression and function of Robos and Slits. *J. Neurosci.* 20, 4975–4982.

Garrity, P.A., Rao, Y., Salecker, I., McGlade, J., Pawson, T., and Zipursky, S.L. (1996). *Drosophila* photoreceptor axon guidance and targeting requires the Dreadlocks SH2/SH3 adapter protein. *Cell* 85, 639–650.

Hall, A. (1998). Rho GTPases and the actin cytoskeleton. *Science* 279, 509–514.

Higgs, H.N., and Pollard, T.D. (2000). Activation by Cdc42 and PIP2 of Wiskott-Aldrich Syndrome protein (WASP) stimulates actin nucleation by Arp2/3 complex. *J. Cell Biol.* 150, 1311–1320.

Hildebrand, J.D., Taylor, J.M., and Parsons, J.T. (1996). An SH3 domain-containing GTPase-activating protein for Rho and Cdc42 associates with focal adhesion kinase. *Mol. Cell. Biol.* 16, 3169–3178.

Hing, H., Xiao, J., Harden, N., Lim, L., and Zipursky, S.L. (1999). Pak functions downstream of Dock to regulate photoreceptor axon guidance in *Drosophila*. *Cell* 97, 853–863.

Hu, H. (1999). Chemorepulsion of neuronal migration by Slit2 in the developing mammalian forebrain. *Neuron* 23, 703–711.

Huang, Y.-Z., Won, S., Ali, D.W., Wang, Q., Tanowitz, M., Du, Q.-S., Pelkey, K.A., Yang, D.J., Xiong, W.C., Salter, M.W., and Mei, L. (2000). Regulation of neuregulin signaling by PSD95 interacting with ErbB4 at CNS synapses. *Neuron* 26, 443–455.

Jin, Z., and Strittmatter, S.M. (1997). Rac1 mediates Collapsin-1-induced growth cone collapse. *J. Neurosci.* 17, 6256–6263.

Kidd, T., Brose, K., Mitchell, K.J., Fetter, R.D., Tessier-Lavigne, M., Goodman, C.S., and Tear, G. (1998). Roundabout controls axon crossing of the CNS midline and defines a novel subfamily of evolutionarily conserved guidance receptors. *Cell* 92, 205–215.

Kidd, T., Bland, K.S., and Goodman, C.S. (1999). Slit is the midline repellent for the Robo receptor in *Drosophila*. *Cell* 96, 785–794.

Kuhn, T.B., Brown, M.D., Wilcox, C.L., Raper, J.A., and Bamberg, J.R. (1999). Myelin and collapsin-1 induce motor neuron growth cone collapse through different pathways: inhibition of collapse by opposing mutants of Rac1. *J. Neurosci.* 19, 1965–1975.

Lamarque, N., and Hall, A. (1994). GAPs for rho-related GTPases. *Trends Gen.* 10, 436–440.

Li, H.S., Chen, J.H., Wu, W., Fagaly, T., Zhou, L., Yuan, W., Dupuis, S., Jiang, Z.H., Nash, W., Gick, C., et al. (1999). Vertebrate slit, a secreted ligand for the transmembrane protein roundabout, is a repellent for olfactory bulb axons. *Cell* 96, 807–818.

Lin, M.Z., and Greenberg, M.E. (2000). Orchestral maneuvers in the axon: Trio and the control of axon guidance. *Cell* 101, 239–242.

Luo, L. (2000). Rho GTPases in neuronal morphogenesis. *Nature Rev. Neurosci.* 1, 173–180.

Ma, L., Rohatgi, R., and Kirschner, M.W. (1998). The Arp2/3 complex mediates actin polymerization induced by the small GTP-binding protein Cdc42. *Proc. Natl. Acad. Sci. USA* 95, 15362–15367.

Machesky, L.M., and Insall, R.H. (1999). Signaling to actin dynamics. *J. Cell Biol.* 146, 267–272.

Miki, H., Miura, K., and Takenawa, T. (1996). N-WASP, a novel actin-depolymerizing protein, regulates the cortical cytoskeletal rearrangement in a PIP2-dependent manner downstream of tyrosine kinases. *EMBO J.* 15, 5326–5335.

Miki, H., Sakai, T., Takai, Y., and Takenawa, T. (1998). Induction of filopodium formation by a WASP-related actin-depolymerizing protein N-WASP. *Nature* 391, 93–96.

Mueller, B.K. (1999). Growth cone guidance: first steps towards a deeper understanding. *Annu. Rev. Neurosci.* 22, 351–388.

- Mullins, R.D., and Pollard, T.D. (1999). Rho-family GTPases requires Arp2/3 complex to stimulate actin polymerization in *Acanthamoeba*. *Curr. Biol.* 9, 405–415.
- Mullins, R.D., Heuser, J.A., and Pollard, T.D. (1998). The interaction of Arp2/3 complex with actin: nucleation, high affinity pointed end capping, and formation of branching networks of filaments. *Proc. Natl. Acad. Sci. USA* 95, 6181–6186.
- Nguyen Ba-Charvet, K.T., Brose, K., Marillat, V., Kidd, T., Goodman, C.S., Tessier-Lavigne, M., Sotelo, C., and Chedotal, A. (1999). Slit2-Mediated chemorepulsion and collapse of developing forebrain axons. *Neuron* 22, 463–473.
- Nguyen Ba-Charvet, K.T., Brose, K., Ma, L., Wang, K.H., Marillat, V., Sotelo, C., Tessier-Lavigne, M., and Chedotal, A. (2001). Diversity and specificity of actions of Slit2 proteolytic fragments in axon guidance. *J. Neurosci.* 21, 4281–4289.
- Niclou, S.P., Jia, L., and Raper, J.A. (2000). Slit2 is a repellent for retinal ganglion cell axons. *J. Neurosci.* 20, 4962–4974.
- Nüsslein-Volhard, C., Wieschaus, E., and Kluding, H. (1984). Mutations affecting the pattern of the larval cuticle in *Drosophila melanogaster*. I. Zygotic loci on the second chromosome. *Roux's Arch. Dev. Biol.* 193, 267–282.
- O'Brien, S.P., Seipel, K., Medley, Q.G., Bronson, R., Segal, R., and Streuli, M. (2000). Skeletal muscle deformity and neuronal disorder in Trio exchange factor-deficient mouse embryos. *Proc. Natl. Acad. Sci. USA* 97, 12074–12078.
- Paulus, W., Baur, I., Boyce, F.M., Breakfield, X.O., and Reeves, S.A. (1996). Self-contained, tetracycline-regulated retroviral vector system for gene delivery to mammalian cells. *J. Virol.* 70, 62–67.
- Pear, W., Scott, M., and Nolan, G.P. (1997). Generation of high titer, helper-free retroviruses by transient transfection. In *Methods in Molecular Medicine: Gene Therapy Protocols*, P. Robbins, ed. (Humana Press, Totowa, NJ), pp. 41–57.
- Prehoda, K.E., Scott, J.A., Mullins, R.D., and Lim, W.A. (2000). Integration of multiple signals through cooperative regulation of the N-WASP-Arp2/3 complex. *Science* 290, 801–806.
- Ren, X.-D., Kiousses, W.B., and Schwartz, M.A. (1999). Regulation of the small GTP-binding protein Rho by cell adhesion and the cytoskeleton. *EMBO J.* 18, 578–585.
- Ren, X.R., Du, Q.-S., Huang, Y.-Z., Ao, S.-Z., Mei, L., and Xiong, W.-C. (2001). Regulation of CDC42 GTPase by Proline-rich tyrosine kinase 2 interacting with PSGAP, a novel Pleckstrin Homology and Src Homology 3 domain containing rhoGAP protein. *J. Cell. Biol.* 152, 971–984.
- Ridley, A., and Hall, A. (1992). The small GTP-binding protein Rho regulates the assembly of focal adhesions and actin stress fibers in response to growth factors. *Cell* 70, 389–399.
- Ringstedt, T., Braisted, J.E., Brose, K., Kidd, T., Goodman, C., Tessier-Lavigne, M., and O'Leary, D.D.M. (2000). Slit inhibition of retinal axon growth and its role in retinal axon pathfinding and innervation patterns in the diencephalon. *J. Neurosci.* 20, 4983–4991.
- Rohatgi, R., Ma, L., Miki, H., Lopez, M., Kirchhausen, T., Takenawa, T., and Kirschner, M.W. (1999). The interaction between N-WASP and the Arp2/3 complex links Cdc42-dependent signals to actin assembly. *Cell* 97, 221–231.
- Rohatgi, R., Ho, H.H., and Kirschner, M.W. (2000). Mechanism of N-WASP activation by CDC42 and phosphatidylinositol 4,5-bisphosphate. *J. Cell Biol.* 150, 1299–1309.
- Rothberg, J.M., Hartley, D.A., Walther, Z., and Artavanis-Tsakonas, S. (1988). Slit: an EGF-homologous locus of *D. melanogaster* involved in the development of the embryonic central nervous system. *Cell* 55, 1047–1059.
- Ruan, W., Pang, P., and Rao, Y. (2000). The SH2/SH3 adaptor protein Dock interacts with the Ste20-like kinase misshapen in controlling growth cone motility. *Neuron* 24, 595–605.
- Sander, E.E., van Delft, S., ten Klooster, J.P., Reid, T., van der Kammen, R.A., Michiels, F., and Collard, J.G. (1998). Matrix-dependent Tiam1/Rac signaling in epithelial cells promotes either cell-cell adhesion or cell migration and is regulated by phosphatidylinositol 3-kinase. *J. Cell Biol.* 143, 1385–1398.
- Shamah, S.M., Lin, M.Z., Goldberg, J.L., Estrach, S., Sahin, M., Hu, L., Bazalakova, M., Neve, R.L., Corfas, G., Debant, A., and Greenberg, M.E. (2001). EphA receptors regulate growth cone dynamics through the novel guanine nucleotide exchange factor ephexin. *Cell* 105, 233–244.
- Swift, S., Lorens, J., Achacoso, P., and Nolan, G.P. (1999). Rapid production of retroviruses for efficient gene delivery to mammalian cells using 293T cell-based systems. In *Current Protocols in Immunology*, J. Coligan, A. Kruisbeek, D. Margulies, E. Shevach, W. Strober, eds. (New York: Wiley), Unit 10.28, Suppl. 31.
- Symons, M., Dery, J.M.J., Karlak, B., Jiang, S., Lemahieu, V., McCormick, F., Francke, U., and Abo, A. (1996). Wiskott-Aldrich Syndrome protein, a novel effector for the GTPase CDC42Hs, is implicated in actin polymerization. *Cell* 84, 723–734.
- Vastrik, I., Eickholt, B.J., Walsh, F.S., Ridley, A., and Doherty, P. (1999). Sema3A-induced growth-cone collapse is mediated by Rac1 amino acids 17–32. *Curr. Biol.* 9, 991–998.
- Vikis, H.G., Li, W., He, Z., and Guan, K.-L. (2000). The semaphorin receptor plexin-B1 specifically interacts with active Rac in a ligand-dependent manner. *Proc. Natl. Acad. Sci. USA* 97, 12457–12462.
- Wahl, S., Barth, H., Ciossek, T., Aktories, K., and Mueller, B.K. (2000). Ephrin-A5 induces collapse of growth cones by activating Rho and Rho kinase. *J. Cell Biol.* 149, 263–270.
- Wang, K.-H., Brose, K., Arnott, D., Kidd, T., Goodman, C.S., Henzel, W., and Tessier-Lavigne, M. (1999). Purification of an axon elongation- and branch-promoting activity from brain identifies a mammalian Slit protein as a positive regulator of sensory axon growth. *Cell* 96, 771–784.
- Wu, W., Wong, K., Chen, J., Jiang, Z., Dupuis, S., Wu, J.Y., and Rao, Y. (1999). Directional guidance of neuronal migration in the olfactory system by the protein Slit. *Nature* 400, 331–336.
- Wu, J.Y., Feng, L., Park, H.-T., Havlioglu, N., Wen, L., Tang, H., Bacon, K.B., Jiang, Z., Zhang, X.-C., and Rao, Y. (2001). The neuronal repellent Slit inhibits leukocyte chemotaxis induced by chemotactic factors. *Nature* 410, 948–952.
- Yuan, W., Zhou, L., Chen, J., Wu, J.Y., Rao, Y., and Ornitz, D. (1999). The mouse Slit family: secreted ligands for Robo expressed in patterns that suggest a role in morphogenesis and axon guidance. *Dev. Biol.* 212, 290–306.
- Zallen, J.A., Yi, B.A., and Bargmann, C.I. (1998). The conserved immunoglobulin superfamily member SAX-3/Robo directs multiple aspects of axon guidance in *C. elegans*. *Cell* 92, 217–227.
- Zigmond, S.H., Joyce, M., Borleis, J., Bokoch, G.M., and Devreotes, P.N. (1997). Regulation of actin polymerization in cell-free systems by GTP $\gamma$ S and Cdc42. *J. Cell Biol.* 138, 363–374.
- Zhu, Y., Li, H.S., Zhou, L., Wu, J.Y., and Rao, Y. (1999). Cellular and molecular guidance of GABAergic neuronal migration from the striatum to the neocortex. *Neuron* 23, 473–485.

#### Accession Numbers

The following accession numbers for mouse srGAPs have been deposited in GenBank: mouse srGAP1, AY057898; mouse srGAP2, AY057899; mouse srGAP3, AY057900.